International Journal of Pharmaceutics 605 (2021) 120793

Contents lists available at ScienceDirect

International Journal of Pharmaceutics

journal homepage: www.elsevier.com/locate/ijpharm

Anti-counterfeiting protection, personalized medicines – Development of 2D identification methods using laser technology

Krisztina Ludasi [a], Orsolya Jójárt-Laczkovich [a], Tamás Sovány [a], Béla Hopp [b], Tamás Smausz [b], Attila Andrásik [b], Tamás Gera [b], Zsolt Kovács [c,d], Géza Regdon jr [a,*]

[a] Institute of Pharmaceutical Technology and Regulatory Affairs, University of Szeged, Eötvös utca 6., 6720 Szeged, Hungary
[b] Department of Optics and Quantum Electronics, University of Szeged, Dóm tér 9., 6720 Szeged, Hungary
[c] Department of Experimental Physics, University of Szeged, Dóm tér 9., 6720 Szeged, Hungary
[d] Department of High Energy Experimental Particle and Heavy Ion Physics, Wigner Research Centre for Physics, Konkoly-Thege Miklós út 29-33., 1121 Budapest, Hungary

ARTICLE INFO

Keywords:
Falsified medicines
Identification
Anti-counterfeiting medicines
Personalized medicines
Laser marking
Unique laser coding

ABSTRACT

Counterfeiting of the products for healing is as old as trading, and it is difficult to quantify the magnitude of the problem. It is known that substandard and/or falsified (SF) medicines are a growing global threat to health, and they cause serious social and economic damage. The EU has a strong legal framework for medicines, it is mandatory to meet the requirements of Directive 2011/62/EU. Serialisation prevents SF medicinal products from entering the legal distribution chain. The present study is an extension of the original idea and aims to develop a laser technology-based method to mark an individual traceable code on the surface of the tablet, which technology can also be used for marking personalized medicines. The method is based on the ablation of the upper layer of a double-layer, differently coloured coating. The 2D code should be formed without harming the functional layer, and anyone with a smartphone integrated with a camera should be able to authenticate these drugs with a suitable application. The present findings confirmed that KrF excimer laser and Ti:sapphire femtosecond laser are efficient and reliable for marking. These should be promising candidates for pharmaceutical companies that would like to have additional protection against drug counterfeiters.

1. Introduction

Counterfeiting of the products for healing is as old as trading, dating back to 1495 BCE, when there was a hunt for genuine medicinal plants at the request of Queen Hatshepsut of Egypt because the market was full of worthless fakes (Brickell, 2001). In the 18th century, when malaria was still endemic in Europe, the continent was flooded with false cinchona bark used to treat fevers (WHO, 2017a).

Substandard and falsified (SF) medicinal products pose a growing threat to public health as they can deliver hazardous treatment or even cause death (Han et al., 2012a). Moreover, in health institutions physicians and pharmacists may not even be aware of patients buying medicines from uncertain or illegal sources, but these products are likely to influence the success of therapies (Fittler et al., 2018b). Bringing these drugs under control is a considerable challenge globally (Han et al., 2012a).

Substandard medicines are authorized medical products that fail to meet either their quality standards or specifications, or both, while falsified medical products are those that deliberately misrepresent their identity, composition or source (WHO, 2017b).

Some falsified medical products are almost visually identical to the genuine product and very difficult to detect. However, many can be identified (WHO, 2018). Possible techniques for detection: **visual analysis** (inspection of packaging condition, labelling, spelling mistakes, dosage units, expiry dates, or various product security features like watermarks, holograms or microprinting, etc.), **physical analysis** (observation of discolourations, surface investigations by microscopy, furthermore, evaluation of disintegration or dissolution measurements, etc.), and **chemical analysis** (classical chemistry or instrumental analysis such as spectroscopy, spectrometry, chromatography, etc.) (Davison, 2011; Roth et al., 2019).

The EU has a strong legal framework for medicines. At the end of the distribution chain, only licensed pharmacies and approved retailers are allowed to sell medicines, including legitimate sale via the Internet

* Corresponding author.
E-mail address: geza.regdon@pharm.u-szeged.hu (G. Regdon jr).

https://doi.org/10.1016/j.ijpharm.2021.120793
Received 10 March 2021; Received in revised form 4 June 2021; Accepted 7 June 2021
Available online 10 June 2021
0378-5173/© 2021 The Authors. Published by Elsevier B.V. This is an open access article under the CC BY license (http://creativecommons.org/licenses/by/4.0/).

(European Medicines Agency, 2018a). For EU Member States, since February 2019, it has been mandatory to satisfy the requirements of Commission Delegated Regulation (EU) 2016/161(European Commission, 2015) and Directive 2011/62/EU (The European Parlament and the Council of the European Union, 2011) of June 2011. Serialisation prevents SF medicinal products from entering the legal distribution chain. It involves tracing an individual product from the manufacturer through the wholesaler to the patient, by a unique 2D identification that is put on each box of prescription drugs. The 2D code should include the product code, the batch number, the serial number, the expiry date, and the national identification number if required by the Member State where the product is placed on the market (European Commission, 2015). In order to combat drug counterfeiting, pharmaceutical manufacturers and suppliers are working on adopting a worldwide standardized identification system (Trenfield et al., 2019).

The aim of this research is to support the regulation and to develop a technology for marking an individual traceable code directly on the surface of the medicine. Oral drug delivery is the most preferred and convenient route of drug administration (Viswanathan et al., 2017), and from among these, tablets are the most chosen pharmaceutical drug delivery systems. They are physically and chemically stable during storage, simple-to-use, have sustainable production and generally excellent content uniformity (Haaser et al., 2013). Therefore, tablets were chosen for marking in this study. The laser coding technology allows the authentication of tablets and avoids illegal repackaging.

For encoding, the Quick Response (QR) Code was chosen, which contains information in vertical and horizontal directions. It offers high-capacity encoding so it can hold a great volume of information. QR codes have different features and data capacities. Some have a maximum storing capacity of approximately 7000 figures (Denso Wave, 1994). They have an error correction capability that can restore data from a partially damaged code, and they offer omnidirectional reading. Because of these features, the QR code is suitable for encoding a high-level authentication capability (Han et al., 2012b). In the case of tablets, it is possible to encode in the QR code the name of the drug or information relevant to the patient, the usage, the dose, the ID of the producer and the batch number or the expiration date, etc. (Edinger et al., 2018). Further research is needed to determine the maximum information density of QR codes produced by the laser ablation technique on curved drug surfaces. In 2018, the European Medicines Agency (EMA) published a guideline on the use of mobile scanning and other technologies, such as QR coding in labelling and packaging of medicines (European Medicines Agency, 2018b).

If marking of individual tablets is aimed at or necessary, the following cases should be considered when laser coding is applied: if the tablets to be marked do not have a coating, at least one coloured layer should be applied to the drug so that the laser coding process can be performed on the surface. In cases when tablets have a coloured coating (for example, for improved swallowability or identification purposes), that layer could be marked. When a functional coating is needed because of the therapy, an extra coating is required on top of it to enable marking without the loss of coating functionality.

In our previous study, the results demonstrated that marking functional coatings by ArF 193 nm excimer laser caused no structural damage in the treated films (Ludasi et al., 2018), although titanium dioxide particles remained in the film during ablation. Those white particles made the accurate reading of the QR codes difficult due to the reduced contrast. To eliminate the problem, naturally coloured coatings were used (Ludasi et al., 2019). That solution seemed to work, but since most coatings contain titanium dioxide for better coverage and/or improved photostability, it would greatly restrict the use of this method. So, another solution had to be found. Each material has an ablation threshold, and for successful marking, the threshold value of the material has to be exceeded (Kannatey-Asibu, 2009). The ablation threshold of a substance is determined by several parameters, which are mostly related to the laser beam. These include the repetition rate of the laser (Hz), wavelength, pulse energy and duration, energy density and the absorption properties of the substrate. By selecting the proper laser parameters, the desired ablation depth can be achieved (Elliott, 1995). To solve the difficulty with titanium dioxide, other types of lasers were tested in this study. In the first case, a KrF excimer laser with a higher wavelength (248 nm) (hereinafter: UV248) was chosen, as it was known from previous experience that the excimer laser was safe. Also, the laser exceeded the ablation threshold of titanium dioxide at the wavelength of 248 nm known from the literature (Van Overschelde et al., 2006). In the second case, a near-infrared (800 nm), short pulse femtosecond laser was used. The assumption was if the pulse is ultrashort, the heat effect is negligible, and no or just little chemical or thermal damage occurs during the removal of the material. In addition, it can create very fine structures, it is more accurately adjustable, faster and also cleaner (Steen and Mazumder, 2010).

In the present experiment, tablets (white) were coated with 2 layers of differently coloured coatings. The transparent bottom layer was the functional one, while the red-coloured top layer was applied to enable marking. The 2D codes were drawn by ablating specific parts of the upper coating layer. Anyone with a camera-enabled phone and a suitable application should be able to authenticate these drugs. In addition, as for healthcare it is increasingly important that each patient receive personalized drug therapy instead of a ‘one-size-fits-all’ treatment (Ayyoubi et al., 2021), these codes could be used as a label in personalized medicine.

We would like to emphasize that, in addition to all kinds of protection and coding, the most important strategy that can be adopted for the patients’ safety is to organize communication and education campaigns to inform them and to educate the public on the safe use of Internet pharmacies. People must be taught to be able to differentiate between legal and illegal medication suppliers (Fittler et al., 2018a). Mobile phone applications that recognize information encoded on tablets can dramatically reduce the time for education, especially for the upcoming generation.

2. Materials

2.1. Tablet core and coating materials

The active ingredient of the model tablet was Ibuprofen DC 85 (Ibu, BASF, Germany) 16.66% (w/w), and excipients: microcrystalline cellulose (Vivapur 102, JRS Pharma, Germany) 74.33% (w/w), crospovidone (Kollidon CL-M, BASF, Germany) 5% (w/w), talc (Molar Chemicals, Hungary) 3% (w/w) and magnesium-stearate (Molar Chemicals, Hungary) 1% (w/w) were used as received.

The shape of the tablets was as follows: Nr1 type: round with flat surface and no break line on it (diameter: 12 mm, crown height: 4.1 mm, average weight: 600 mg). Nr 2 type: round with flat surface and no break line on it (diameter: 10 mm, crown height: 3.1 mm, average weight: 300 mg). Nr 3 type: round with flat surface and no break line on it (diameter: 10 mm, crown height: 4.8 mm, average weight: 500 mg).

Placebo tablets were also used as coating aid for reasons of saving time and material. The placebo tablets were round with biconvex surface and had no break line on them (diameter: 10 mm, crown height: 4.2 mm, average weight: 350 mg).

The first (functional) film-forming agent was an aqueous-based enteric coating dispersion: Eudragit L30 D55® (Evonik Nutrition & Care, Germany). The second film-forming substance was a hydroxypropyl–methylcellulose (HPMC)-based coating formula, Sepifilm PW Red (Seppic S.A., France).

3. Methods

The ingredients of the tablet were homogenized with a Turbula mixer (Willy A. Bachofen Maschienenfabrik, Switzerland) for 8 min, and 2 min after the addition of the lubricant. The homogenous powder

mixture was compressed with a Korsch EK0 (E. Korsch Maschienenfabrik, Germany) single punch eccentric tablet press.

3.1. Coating procedure

330 g of placebo tablets and 70 g of API (Active Pharmaceutical Ingredient) containing tablets were coated together at the same time in order to save material and time.

Eudragit® L30-D55 aqueous polymer dispersion was prepared. It consisted of 16.76% w/w dry substance of a methacrylic acid - ethyl acrylate copolymer with a ratio of 1:1 (dispersion 30% w/w) (Evonik Nutrition & Care GmbH), PlasAcryl® HTP 20 (Evonik Nutrition & Care GmbH) 2.9% w/w dry substance was added to the dispersion as plasticizer/anti-tacking agent and distilled water 1 h before coating.

The aqueous HPMC coating solutions consisted of 20% w/w dry substance in the case of Sepifilm™ PW Red coating system. According to the supplier's recommendation, they were dispersed in purified water. The total mixing time took 45 min, followed by sieving the dispersion through a 0.5 mm sieve.

Spray coating was performed in a 4 M8 Pancoat (ProCepT, Belgium) perforated coating pan. 2 layers of coatings were put on the tablets. The first layer was Eudragit L30 D55. A 0.8 mm spray nozzle was used for the application of the atomised spray coating solution for 75 min, with an atomising air pressure of 1.0 bar, a spray rate of 3 g/min and an air flow rate of 0.70 m^3/min. The drying and cooling process lasted for 15 min. Other coating parameters are shown in Table 1.

The second layer was the HPMC-based ready-to-use coating formula. A 0.8 mm spray nozzle was used for the application of the atomised spray coating solution for 45 min in the case of Sepifilm PW coating, with an atomising air pressure of 2.0 bars, a spray rate of 2 g/min and an air flow rate of 0.70 m^3/min. The drying and cooling process lasted for 15 min. Other coating parameters for the second layer are shown in Table 2.

The final coating thickness was measured with a stereomicroscope (Zeiss, Germany). Measurements were performed at a magnification of 500. After calibration, 4–4 tablets were examined, which were cut in half along the middle of the tablet band, and each was measured at 10 places and averaged.

3.2. Irradiation of coated tablets

2 different types of lasers were used for the irradiation of the tablets. The experimental setup for the laser processing is outlined in Fig. 1.

KrF excimer laser (UV248) was used for the UV-regime ablation, a twin-tube hybrid dye-excimer laser-system (Szatmári, 1994, Szatmári and Schäfer, 1988). The current laser setup produced 60 mJ laser pulses with a pulse length of 700 fs. The central part of unfocused 4 cm × 4 cm pulses was cut out by an aperture 2 cm in diameter and the remaining pulses were attenuated with dielectric coated plates to about 1–2 mJ in order to avoid plasma formation in the air. The parameters of irradiation using excimer laser were the following: wavelength: 248 nm, energy: 0.5 mJ, number of impulses: 10, spot size: 100 μm, FWHM: 700 fs, fluence: 6.37 J/cm^2.

Ti:sapphire Femtosecond laser (Femto), operating in the TeWaTi laser lab at the University of Szeged (TeWaTi, 2019) provided amplified pulses with a repetition rate of 200 Hz and maximum pulse energy of 1 mJ. An achromatic lens with a focal length of 150 mm focused the beam onto the target placed into the focal plane, allowing beam imaging of f/19 (F-number) and processing of the target surface with 135 fs pulses. Irradiation of tablets using Femto laser: wavelength: 800 nm, energy: 0.62 mJ, number of impulses: 20, spot size: 110 μm, FWHM: 135 fs, repetition rate: 200 Hz, fluence: 6.52 J/cm^2.

A computer-controlled, movable desktop, a motorized translator was created to be able to change the position of the tablet during lasering (Fig. 1). The QR code was ablated hole by hole. During UV248 laser ablation, the oval-shaped holes in the film followed the shape of the beam. It took 1.5–2 h to create such a code with the UV248 laser and 10 mins with the Femto laser.

Table 1
Coating parameters of Eudragit L30 D55.

Step	Inlet air temperature (°C)	Exhaust air Temperature (°C)	Tablet temperature (°C)	Drum speed (rpm)
Warm-up	60		Until 50	3
Coating	45–55	40–45	30–35	15
Drying	50	38–40	35–37	3
Cooling	25	25	25	3

Table 2
Coating parameters of Sepifilm films.

Step	Inlet air temperature (°C)	Exhaust air Temperature (°C)	Tablet temperature (°C)	Drum speed (rpm)
Warm-up	60		Until 50	3
Coating	55	40–42	35	9
Drying	40	30	27	3
Cooling	25	25	25	3

3.3. Surface profilometer

Veeco, Dektak 8 Advanced Development Profiler® was used for profilometry measurements. The tips employed had a radius of curvature ~2.5 μm, and the force applied to the surface during scanning was ~30 μN. The horizontal resolution was 0.1–0.13 μm, and the vertical resolution was 40 Å. Dektak software (Microsoft® Windows XP®: interactive data acquisition) and Vision® 32 software (data processing, 2D and 3D image analysis) were used for data evaluation (Veeco Instruments Inc., New York, USA).

3.4. Determination of the ablation threshold

The characteristics of the ablation holes were examined with a surface profilometer. The laser parameters required for ablation were determined from the data obtained using a profilometer according to the method described below.

The ablation threshold indicates the minimal laser energy required to remove the material from the substrate (i.e., tablet surface). The threshold value is a fundamental parameter for laser fine-tuning. In most of the cases, the laser operates close to the threshold but with slightly higher energy to avoid unwanted side effects, such as the thermal distortion of the material. The final etching depth is controlled by the number of laser impulses and not by fluence (Lawrence, 2010).

As the spatial distribution of fluence was different for the two laser types (homogeneous flat top and Gaussian), two different methods were applied to determine the corresponding ablation threshold.

The first method is based on the measured ablation rate (ablation depth per number of laser impulses). The ablation rate shows a logarithmic correlation with the applied fluence (impulse total energy per unit surface area) close to the threshold. The $l = (1/\alpha)\ \ln(F/F_{th})$ logarithmic function was fitted to the measurements by using nonlinear least-squares (NLLS) Marquardt-Levenberg algorithm in this case.

The second method is based on the measured ablation diameter. The linearized model log(energy) versus estimated impact surface was used in this case to calculate the zero crossing by fitting the linear trend to the measurements.

Fig. 2 summarizes the threshold calculation results for the UV248 laser. Only the first method was used for threshold estimation in this case. Fig. 3 shows the results for the Femto laser, where the second method was used for threshold estimation in two measurement sessions.

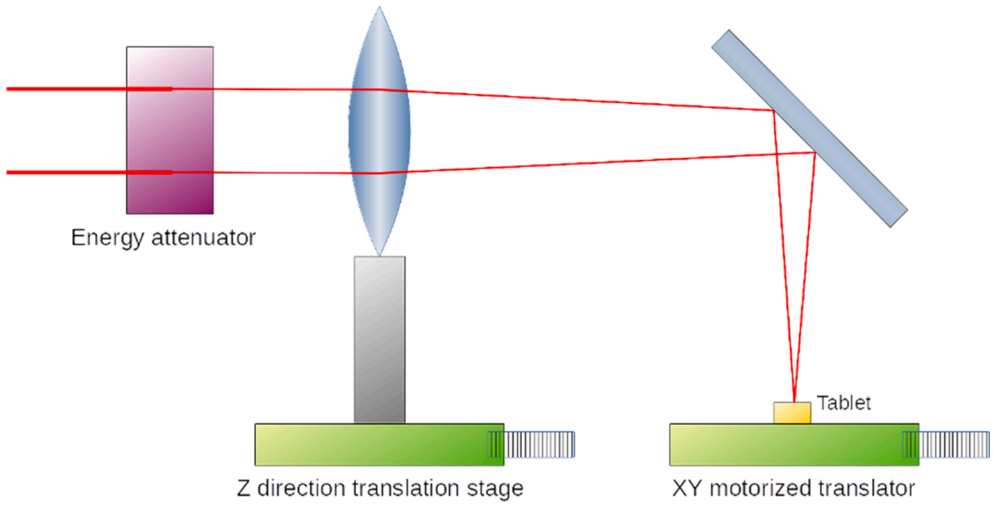

Fig. 1. Experimental setup for laser processing. The tablet position was adjusted with a motorized XY translator during the QR code engraving. The Z direction translator stage was used to set the focus plane precisely on the surface of the tablet.

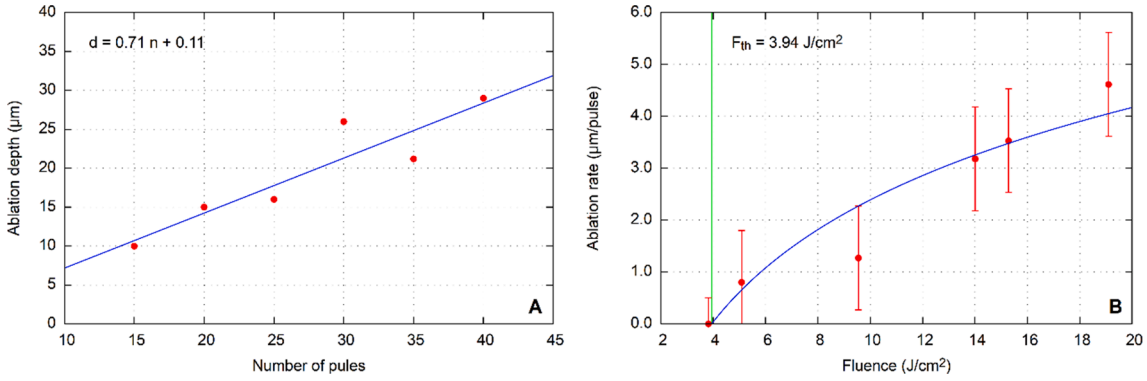

Fig. 2. UV248 laser ablation threshold determination. A: Ablation depth estimation based on the number of the applied laser pulses. B: Threshold calculation result based on ablation depth by using logarithmic model fit.

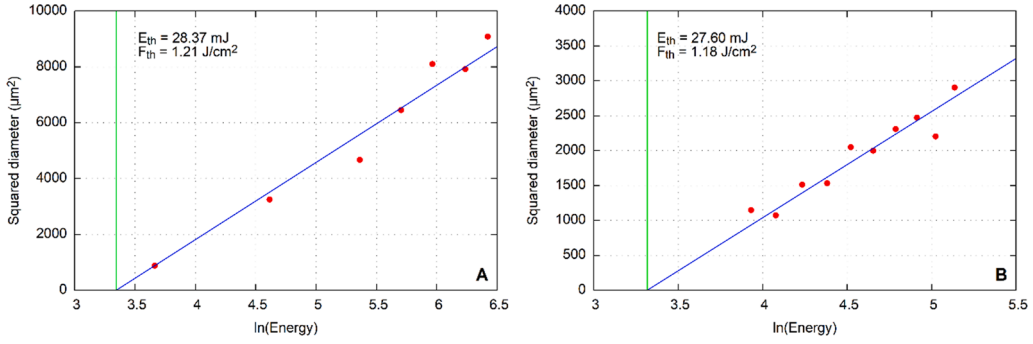

Fig. 3. Femto laser ablation threshold determination. A, B: Threshold calculation result based on ablation diameter using a linearized model. Diagrams A and B represent two measurement sets with different pulse energy ranges.

3.5. Scanning electron microscope (SEM)

The ablated tablet was observed by using a scanning electron microscope (SEM, Hitachi, Japan S4700). The tablets were mounted rigidly on a specimen holder with a double-sided carbon adhesive tape and a conductive ultrathin golden layer was deployed on them with a sputter device (Polaron, UK). The measurements were performed at a magnification of 30–5000, applying 10.0 kV electron energy and 1.3–13 MPa air pressure.

3.6. Raman spectra

Raman spectroscopy was used for the examination of the tablets treated by lasers. Spectra were acquired with a Thermo Fisher DXR Dispersive Raman spectrometer (Thermo Fisher Scientific Inc., MA, USA), a diode laser operating at a wavelength of 780 nm and equipped with a CCD camera. Raman measurements were carried out with a laser power of 4 mW (Ibu) and 12 mW (Eudragit L30 D55, Sepifilm PW Red) at a slit aperture size of 25 µm. The spectra of the tablets treated by lasers were collected by using an exposure time of 6 sec, and 10 spectra were

averaged in the spectral range of 3200–200 cm^{-1} with cosmic ray and fluorescence corrections.

Raman chemical mapping was also performed with the same equipment. Spectral data were collected on the surface of the lasered tablet, and on the fracture surface of the halved tablet, including the treated and the intact region, too. The spectra were determined at certain points in a defined area, while the sample had a translational motion between each discrete measurement. The point scan system measures each spectrum individually at a series of predefined points. The chemical map was profiled to the spectra of Eudragit L30 D55 and to the spectra of Sepifilm PW Red. In the case of Ibu, profiling was made to the peak at 1604 cm^{-1} because it was found to be the most typical for the API, and it was the most separated from the spectra of the other investigated components.

Furthermore, sample analyses were performed on the cross-section surface of both types of laser-treated tablets (10 points directly below the lasered coated surface and 10 points in the core of the lasered tablets). The mean of these 10 spectra was compared with the mean of the 10 spectra taken from the core of the untreated tablet and the spectrum of Ibu. These averaged spectra were normalized to peak 1604 cm^{-1} of the Ibu spectrum.

Data was evaluated with Spectragryph - optical spectroscopy software (F. Menges, 2020).

3.7. In vitro drug disintegration

In the disintegration studies, the tablets were tested according to the standard method of the European Pharmacopoeia with an Erweka model ZT71 apparatus (Erweka, Germany). First, 900 ml of artificial enzyme-free gastric juice (pH = 1.22) was preheated and maintained at a temperature of 37 ± 0.5 °C. According to the guideline, enteric coating should be intact for 2 h in acidic media. After 2 h, the medium was changed to a phosphate buffered saline solution (pH = 6.82). The time necessary for each tablet to disintegrate in acidic and intestinal solution was recorded automatically by the apparatus.

3.8. In vitro drug dissolution

In the present study, the investigation of drug release kinetics from marked tablets was carried out with an Erweka DT 700 (Erweka GmbH, Germany) dissolution tester according to the standards of the European Pharmacopoeia. A rotating basket method was used for the dissolution tests, where the rotation speed was 100 rpm, the dissolution medium was 900 ml of artificial enzyme-free gastric juice (pH = 1.22) for 2 h, and then it was replaced with 900 ml of phosphate buffered saline solution (pH = 6.82) for 1 h. The pH value was checked with a pH meter. The temperature was maintained at 37 ± 0.5 °C. As a sample, 5 ml of the dissolution medium was taken manually at predetermined intervals without being replaced. Medium loss was not taken into account during the calculations. Samples were filtered through a 10 μm Poroplast filter (Erweka, Germany). The absorbance of ibuprofen DC85 was analyzed at 222 nm, using a spectrophotometer (Genesys 10S UV–VIS, Thermo Fisher Scientific Inc., MA, USA). Four tablets were tested, and samples were taken at the following time intervals: at 120 min in the case of gastric juice, and after changing to intestinal fluid at 5, 10, 15, 30, 45 and 60 min.

4. Results and discussion

The present study focuses on demonstrating the effectiveness of a QR code-based authentication process of film-coated tablets, from the formulation of the QR-coded tablets by laser ablation to the decoding step using a QR code reader application on a smartphone.

The primary focus was on removing the titanium dioxide particles that remained in the film during previous ablation studies (Ludasi et al….) by comparing the effectiveness of two different types of lasers in marking. The 2D codes were formed by removing particular parts of the upper coloured coating. After marking, a detailed quality analysis was made to check if any change occurred in the quality of films or in the API during the laser intervention. Also, the disintegration and dissolution of the lasered products were investigated to confirm that it was possible to mark the tablets with functional coating without damaging them during the procedure.

4.1. Microscopic analysis of the coated surface

The QR code (Fig. 4A) that was lasered on the tablets was generated by the QR code generator library libqrencode. (Fukuchi, 2020). A simple code (with content: 12345678) was made as the secondary aim was to find out if it was possible to ablate a decodable QR code on the surface of the tablet by these lasers. Further research is being done on how much information can be encoded in a QR code of a given size to keep the decoding accuracy.

The present study confirmed that titanium dioxide particles did not interfere with decoding when coding had been done by UV248 or Femto lasers. The QR codes applied on the tablets are readable by a smartphone with QR code scanner applications downloaded from the Internet, for example, with QRbot (https://qrbot.net/) or with the photo mode of the mobile phone. The only requirement is that the application must be able to read the “inverse” QR code (Fig. 4B), as in this case the tablet is coloured and the ablated part is white, just the opposite of the usual QR codes.

The results of the UV248 laser treatment are seen in Fig. 5. It can be observed through visual inspection that the 5 × 5 mm QR code is made up of dots.

It is known that a usable QR code can also be created by not overlapping parts, such as dots. The UV248 laser-ablated oval-shaped holes in the film were in accordance with the shape of the beam. It was possible to make a readable code from oval-shaped holes, too, even in cases where laser irradiation was not perfect, as the code has error correction capability that can restore the missing data, as seen on the ablated QR code that is made up of individual points (Fig. 5B,D). Better coverage can be obtained by overlapping the holes, which results in a more readable code. Nevertheless, care must be taken not to punch through the Eudragit layer. The depth of ablation can be controlled by changing the number of pulses on the sample place or the fluence, which allows the accurate setting of the penetration depth to the coating layer. It took 1.5 and 2 h to create such a code by the UV 248 laser depending on whether there was an overlap between the holes or not. Fewer shots mean faster but still effective marking.

The same computer-controlled movable desktop was coupled with the Femto laser to mark the tablet, as in the previous case. At this time, the shape of the beam was round, thus the ablated holes were too, and they overlapped, as shown in Fig. 6. The ablation of the QR code took about 10 min, as the most important limiting factor of overall ablation is the repetition rate of the laser. Therefore, the higher frequency (200 Hz) of the Femto laser dramatically shortens the marking procedure.

Fig. 7A–C displays the scanning electron micrographs of the 4 × 4 mm QR code on the tablet treated by the UV248 laser.

Fig. 7A shows a part of the QR code on the tablet surface, and it is

Fig. 4. Sample QR code ablated on the tablet. A: The common form of the QR code. B: The inverse of the QR code ablated onto the coloured tablet. C: The same QR code but made of dots, prepared for laser and desktop control.

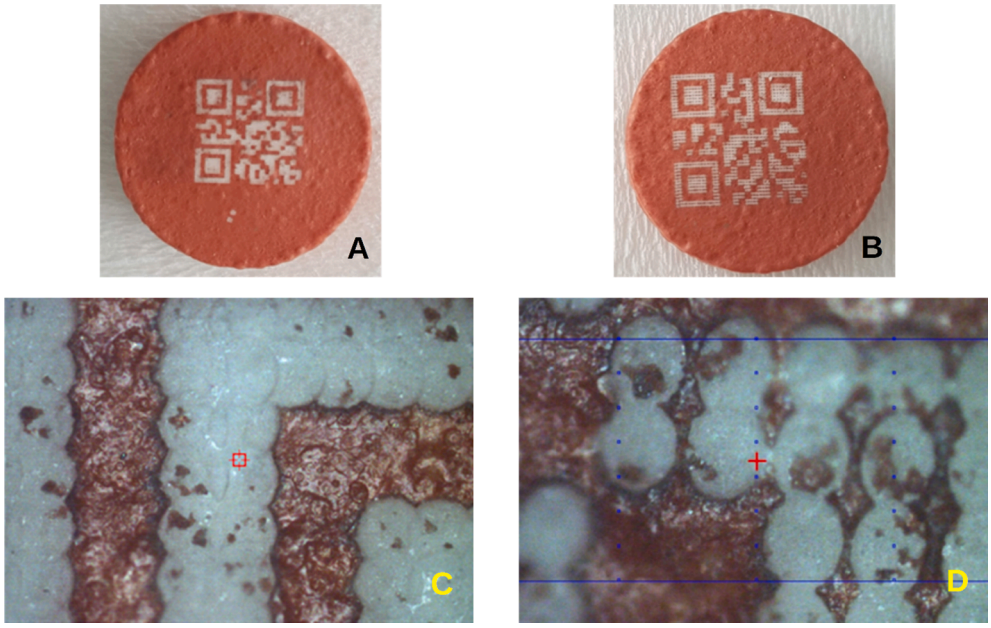

Fig. 5. Tablet encoded by UV248 laser. A: The size of the QR code is 4 × 4 mm. B: The size of the QR code is 5 × 5 mm. C: Microscopic picture of the 4 × 4 mm QR code. D: Microscopic picture of the 5 × 5 mm QR code.

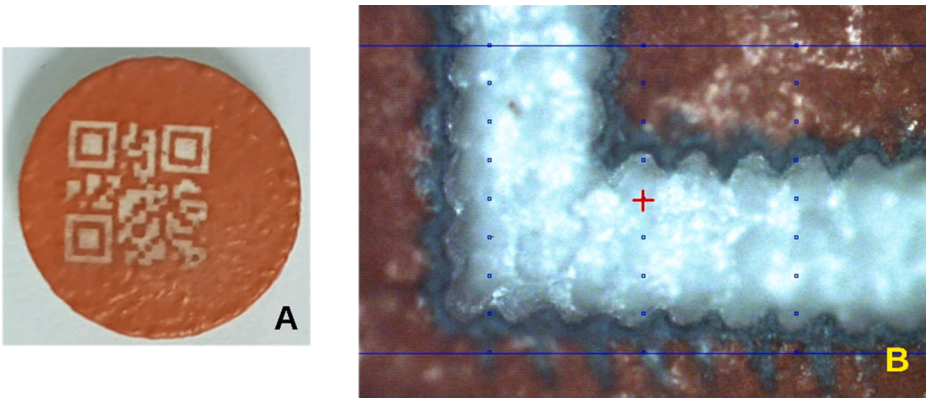

Fig. 6. Tablet encoded by Femto laser. A: Visible to the naked eye. B: Microscopic picture.

clearly visible that it is made of overlapping dots, as described above. The holes are deeper at the overlapping parts. It can also be seen that the surface of the untreated coating is uneven, and the holes visible on the untreated surface may have remained from the bubbles formed during the coating process due to too quick drying since the air did not have time to diffuse out. Fig. 7B displays the lasered tablet surface at greater magnification. The holes in the ablated surfaces could also have resulted from bubble formation. Fig. 7C shows the cross-section surface of the tablet, where the place of lasering is seen in the framed part. The glossy part on the top of the tablet is the PW red coating, which is about 5–10 μm thick. The bottom coating, which is 60–70 μm thick, seems to be intact. The ablated surface of the sample has no large damage. Only a physical change is observed in the structure as a result of the removal of the coating by the UV248 laser, and no obvious sign of chemical change is detected.

Fig. 7D-G displays the micrographs of the Femto lasered tablet. In Fig. 7D, a part of a QR code is seen on a halved tablet. The dots which compose the QR code are clearly visible. The penetration depth seems to be greater with the Femto laser than with the UV248. In Fig. 7E the lasered surface is visible at higher magnification, where intact regions may be identified between the holes. Fig. 7F shows one hole at higher magnification. At the bottom of the ablation cavity a different material is detected, which is thought to be the functional coating because of its different, more porous structure. The laser penetration here seems to have taken place right up to the bottom of the coating. In Fig. 7G, the cross-section surface of the halved tablet is seen. The tablet was fixed to the holder upside down. The ablation area is visible in the framed part. The Femto laser removed the upper coating, which is about 50 μm thick, and in some places, the laser also penetrated into the functional Eudragit coating. Nevertheless, because its thickness is about 150 μm, functionality may still be intact despite its partial absence.

Similarly to the UV248 laser, it may be seen that the Femto laser did not cause considerable damage in the coating structure during the treatment, either. Only a physical change may be detected in the ablated area, fragments of the coating film are visible where the coating was removed. No visible sign of chemical changes was detected in the upper or in the bottom layer. Overall, it can be stated that no visible chemical change occurred on the treated surface when using either of the two lasers.

4.2. Disintegration test

In the disintegration studies, six pieces of coated and ablated tablets were tested from tablet type Nr 3. The tablets remained intact during the

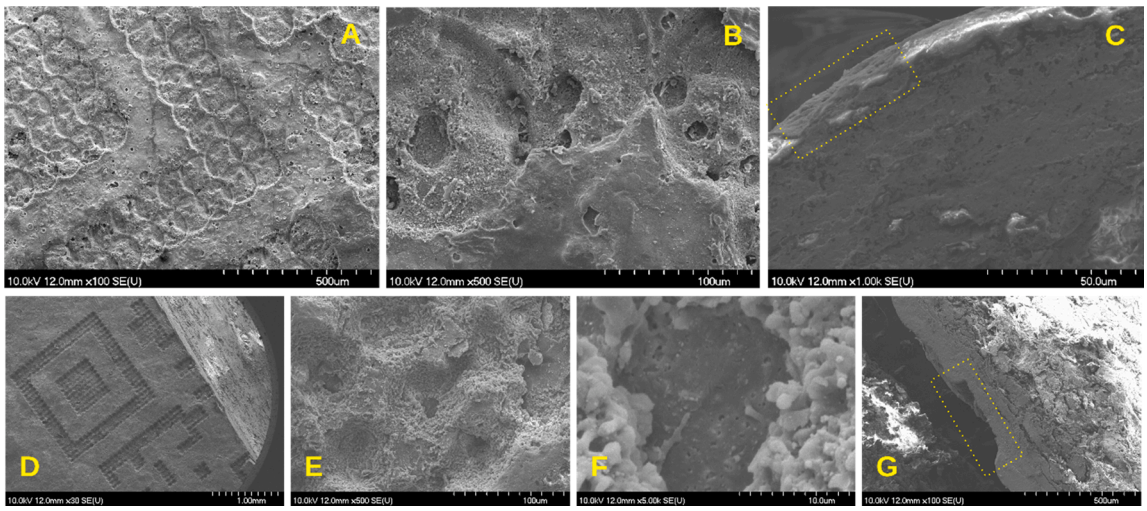

Fig. 7. SEM micrographs of laser-treated tablets. First row: Films A, B, C treated by UV248 laser. A: Tablet surface at a magnification of 100×. B: Tablet surface at a magnification of 500×. C: The tablet's cross-section surface at a magnification of 1000×. Second row: Tablets D, E, F, G treated by Femto laser. D: Tablet surface at a magnification of 30×. E: Tablet surface at a magnification of 500×. F: Ablation hole at a magnification of 5000×. G: The tablet's cross-section surface at a magnification of 100×. C,G: The place of lasering is shown in the framed section.

2-hour disintegration process in the artificial enzyme-free gastric juice, which corresponds to the result expected according to the European Pharmacopoeia, as they had a gastro-resistant coating. After changing to the intestinal fluid, the disintegration test was complete in 30 min for all tablets. This result confirmed our preliminary conclusion based on SEM analysis, according to which the lasering of the upper coating left the functional coating in the bottom intact, and it is possible to mark functionally coated tablets.

4.3. *In vitro drug dissolution test*

For in vitro drug dissolution tests, tablets of different shapes were used: A: Type Nr1, B: Type Nr2, C and D: Type Nr3. Three of the investigated tablets remained intact after 120 min in the gastric medium. The amount of the dissolved API was 0.15%, 2.12%, and 0.92%, for A, C and D, respectively, while the dissolved API was 35.2% for Tablet B, which partially disintegrated during this period.

In order to save time and material, the differently shaped API containing tablets were coated together with placebo tablets. Presumably, due to their different geometry, they were mixed inappropriately during coating, therefore they might have different coating thicknesses. Tablet coating thickness may also vary in the case of identical tablets, as observed by M. Wolfgang et al., where it varied between 56.3 μm and 86.9 μm (Wolfgang et al., 2019). The literature also confirms that the shape of the tablet directly influences intra-tablet coating uniformity. The most likely reason for intra-tablet coating variability is the preferred orientation of tablets when passing through the spray zone of the coater (Wilson and Crossman, 1997). There was another investigation of inter-tablet coating layer thickness, where a comparison of both sides of the tablet surface was made. It shows that the thickness of the coating layer of some tablets on one side of the tablet is up to 10 μm thicker than on the other one (Ho et al., 2007). Achieving a high level of intra-tablet uniformity is especially important for functional film coatings (Dong et al., 2017), where uniform thickness is required to guarantee the desired drug release rate to the patient (Sacher et al., 2019). In the present study, it can be assumed that in the case of tablet B, the coating was thinner and had been damaged during the marking. It is likely that if only tablets of the same shape are coated at a time, the layer thickness will be more uniform and the inner, functional layer can be protected from damage.

The dissolution profile of the tablets in phosphate buffered saline solution is shown in Fig. 8. It can be concluded that during the one-hour

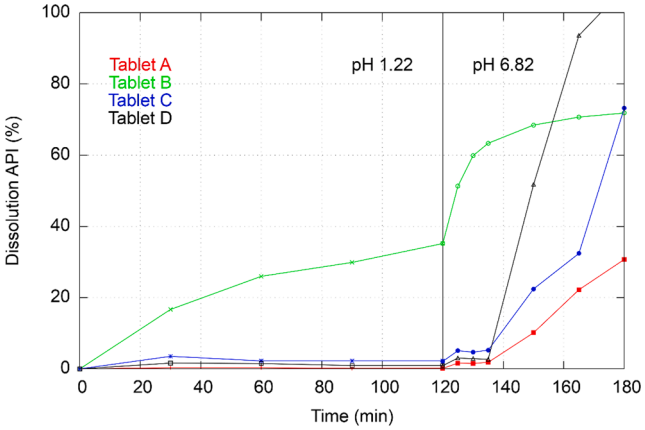

Fig. 8. Drug dissolution curves of the 4 coated and lasered tablets.

in vitro studies, the tablets acted in accordance with pharmacopoeial standards and the disintegration and dissolution process started. It is seen that the dissolution of tablet B started earlier than that of the others, and the final concentration was lower. The explanation for this phenomenon is that the dissolution of tablet B had already started in the gastric medium.

4.4. *Coating film thickness*

To confirm the assumption that not only the inter-tablet but also the intra-tablet variability of final coating thickness is spread over a wide range, microscopic film thickness measurement was applied. Fig. 9 shows the difference in the thickness of the coating on the top and on the side of the tablet. Coating thickness averages measured on different tablets, determined on the basis of measurements at 10 places of 4–4 half tablets, are presented in Table 3.

4.5. *Raman*

Finally, to confirm that the ablation process causes no chemical change, a dispersive Raman spectrometer was used to detect possible changes in the coated tablets. Chemical mapping was chosen to determine if there was a laser-induced change in the coating layers or in the

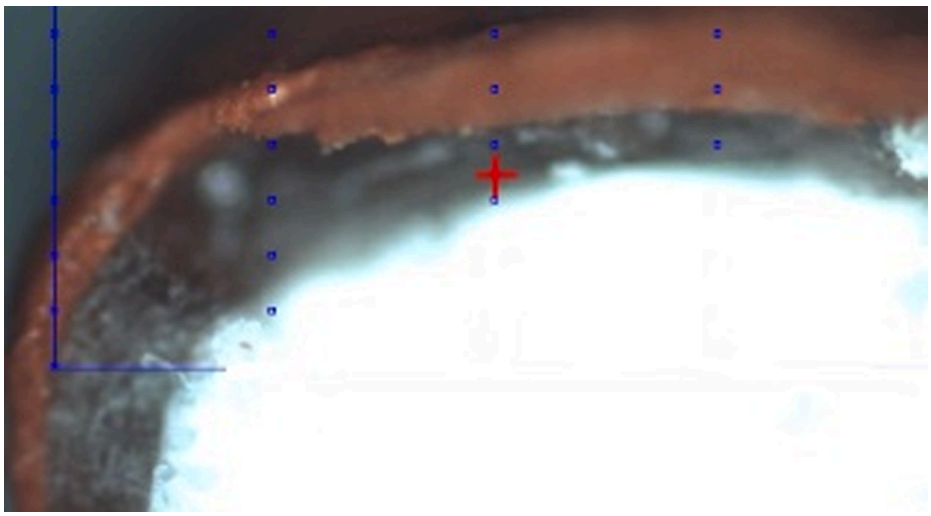

Fig. 9. Uneven thickness of tablet coatings.

Table 3
Thickness of the different coatings.

	12 mm diameter round flat tablet (600 mg)	10 mm diameter round flat tablet (300 mg)	10 mm diameter round flat tablet (500 mg)
PW red coating thickness (μm)	49.43 ± 9.23	16.19 ± 9.19	88.02 ± 18.98
	63.12 ± 14.72	61.78 ± 14.67	95.42 ± 13.45
	59.31 ± 11.82	34.81 ± 11.76	73.26 ± 22.65
	76.75 ± 13.98	45.78 ± 14.56	69.76 ± 16.54
	182.34 ± 22.44	79.62 ± 17.79	155.45 ± 19.57
Eudragit coating thickness (μm)	145.93 ± 29.54	123.65 ± 29.67	98.02 ± 23.77
	204.54 ± 17.57	97.43 ± 23.65	136.23 ± 29.76
	163.78 ± 32.23	134.75 ± 36.76	102.43 ± 13.65

API in the core during marking. The examination was done on the surface of the lasered tablet and on the fracture surface of the halved tablet. The chemical map was profiled based on the spectra that are summarized in Fig. 10. The full spectrum was applied for raw free films (Eudragit L30-D55, Sepifilm PW Red) and a single peak (1604 cm^{-1}) for the API Ibuprofen DC85.

Figs. 11–14 present the data of the obtained chemical maps. Part "A" of the figures shows the microscopic mosaic photo of the laser-treated region, the chemically mapped area is framed with a blue or a red line. The spectra were collected from places marked by blue or red points. The other parts of the Figures show chemical maps, where "B", "C" and "D" show the profiling result of the Eudragit, Ibu and PW red film, respectively. In these maps, warm colours show a higher concentration of the profiled materials. Profiling of the PW red spectrum was performed only for tablet cross-sections.

The UV 248 nm laser-treated tablet surface is presented in Fig. 11 and Fig. 12. The results confirm that the PW red upper layer (Fig. 12D) was completely ablated in the places that were lasered. Based on Fig. 11C, it can be assumed that the laser had reached the API because

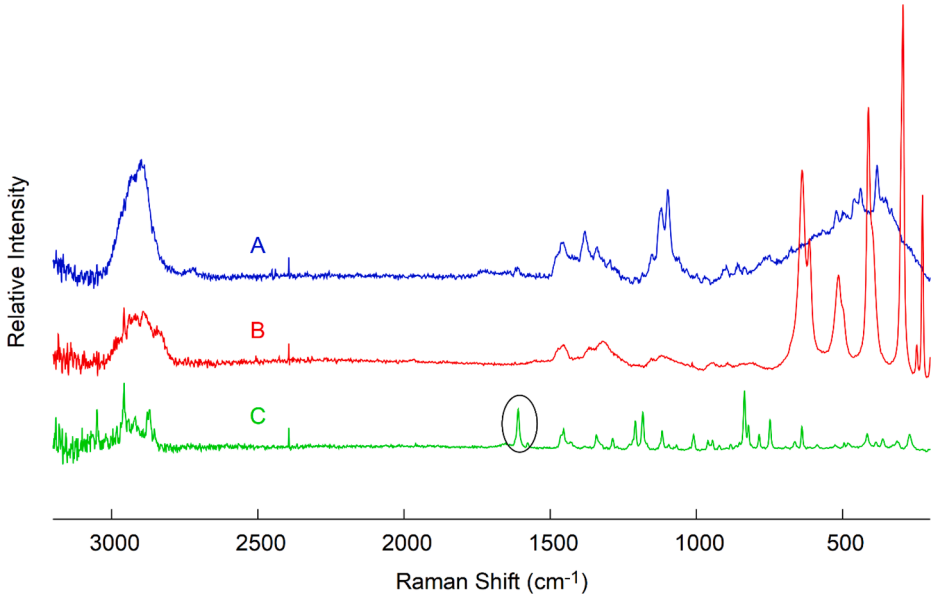

Fig. 10. Raman spectra of film coatings and the API. A: Eudragit L30-D55, B:Sepifilm PW Red, C: API Ibuprofen DC85. Chemical map profiling was performed on spectra A, B and a single peak, which is circled on the spectrum C (1604 cm^{-1}). (For interpretation of the references to colour in this figure legend, the reader is referred to the web version of this article.)

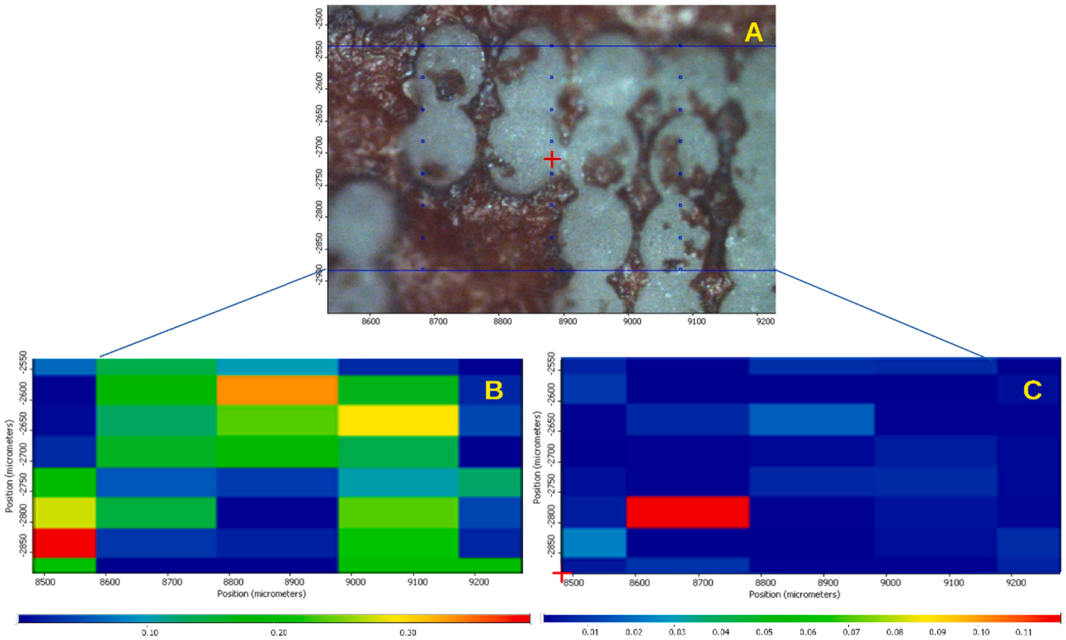

Fig. 11. Surface of the tablet treated by UV248 laser. A: Microscopic picture of the surface of the lasered tablet. B: Chemical map profiled to Eudragit L30-D55. C: Chemical map profiled to Ibu.

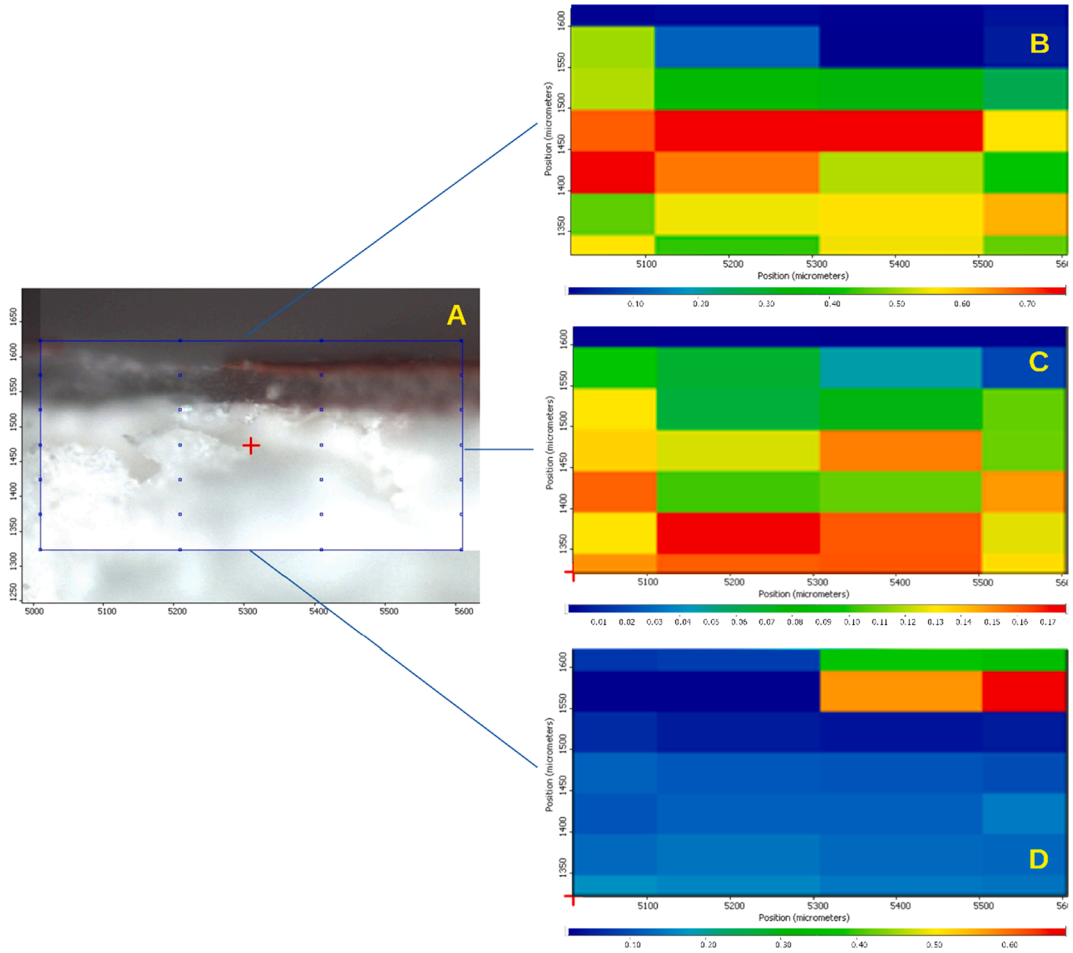

Fig. 12. Fracture surface of a tablet treated by UV248 laser after halving. A: Microscopic picture of the fracture surface of the lasered tablet. B: Chemical map profiled to Eudragit L30-D55. C: Chemical map profiled to Ibu peak. D: Chemical map profiled to Sepifilm PW red. (For interpretation of the references to colour in this figure legend, the reader is referred to the web version of this article.)

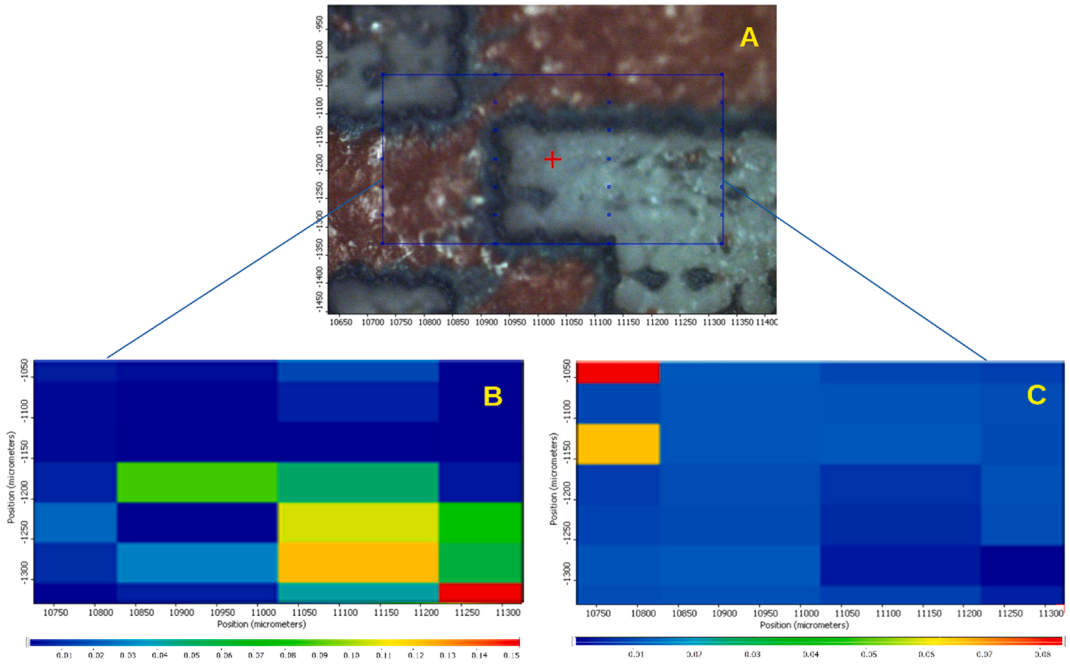

Fig. 13. Surface of the tablet treated by Femto laser. A: Microscopic picture of lasered tablet. B: Chemical map profiled to Eudragit L30-D55. C: Chemical map profiled to Ibuprofen.

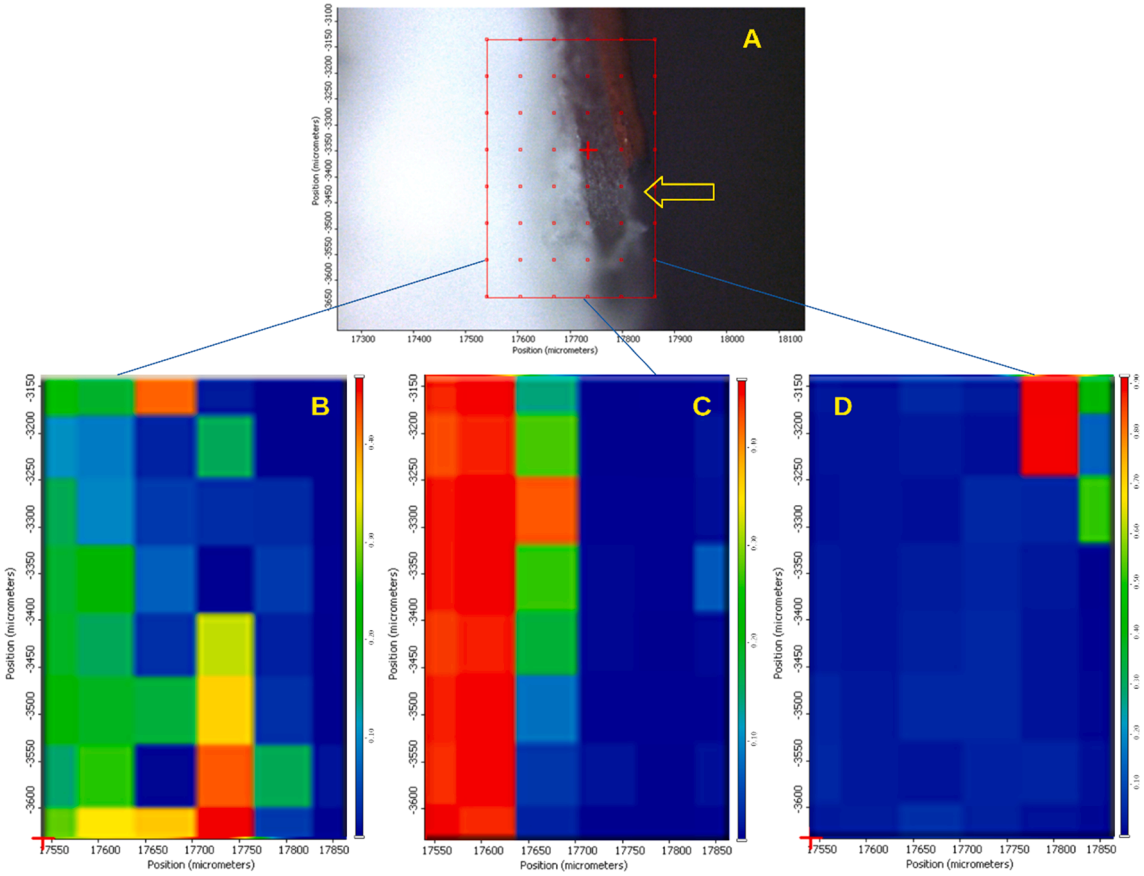

Fig. 14. Cross-section surface of the Femto laser treated tablet. A: Microscopic picture of the halved tablet, arrow pointing at the missing PW red coating. B: Chemical map of the tablet surface profiled to Eudragit L30-D5. C: Chemical map of the tablet surface profiled to Ibuprofen. D: Chemical map of the tablet surface profiled to Sepifilm PW red. (For interpretation of the references to colour in this figure legend, the reader is referred to the web version of this article.)

the thickness of the coating was not consistently even, and furthermore because the API might have penetrated into the Eudragit coating (Fig. 12C).

Fig. 13 and Fig. 14 display the tablet surface and the cross-section of Femto laser-treated tablets, respectively. In Fig. 13B Eudragit is seen in the laser-treated areas, while in Fig. 13C the warm colours show the API Ibu, which suggests that the coating thickness was not consistently even, and the laser might have reached the API or penetrated into the coating in this case as well.

In Fig. 14A the arrow points to the missing PW red coating, and the mapping (Fig. 14D) confirms that it was ablated by the laser. The profiling shows that the API is mostly in the tablet core (Fig. 14C), but in the same picture, the area of the inner coating is green, which means that the API partly migrated from the tablet core to the Eudragit film. According to the literature, such migration during the coating process can happen if the coating is aqueous-based. Migration is enhanced if a component is soluble in the coating solution, and it also depends on the spray conditions used during the coating operation (Dansereau et al., 1993; Guo et al., 2002). Ibu is a Biopharmaceutics Classification System (BCS) class II drug with low solubility at pH = 1.2 and pH = 4.5 but high solubility at pH = 6.8 (Álvarez et al., 2011).

To determine if there was a laser-induced change in the API, Raman measurements were performed on the fracture surface of the tablets treated by the two lasers. Sample analyses were made at 10 points directly below the lasered coating surface and at 10 points in the core of the lasered tablets. As described in the "Methods" section, 10 spectra were averaged at each point. The mean of these spectra was compared with the average of 10 spectra taken from the core of an untreated tablet and with the spectrum of Ibu. These spectra were normalized to peak 1604 cm^{-1} of the Ibu spectrum and are shownin Fig. 15.

There was no significant difference between the spectra taken from the lasered area compared with the spectra taken from the non-lasered area. The most characteristic peaks of Ibu are present in all the spectra, with no slip visible. The observed peak intensities can be attributed to the relative inhomogeneity of the materials in the tablet, depending on how rich or poor Ibu was in the studied region. Sampling with a small laser spot may also result in different intensities due to the inhomogeneous composition of the tablet. It can be stated that no chemical structural change was observed after the labelling. Overall, despite the fact that, mainly due to the uneven thickness of the coating, the laser might occasionally reach the functional coating besides the removal of the PW red layer and also that Ibu may penetrate from the core of the tablet into the functional coating, no chemical structural change was observed in the coatings during labeling.

5. Conclusions

During laser ablation, it is important not to cause any change in the medicine. Commonly, it is the thermal effect which can cause problems in the material's quality. At the same time, the coating has to be removed at specific points. This can be achieved by choosing the right laser and setting the optimal parameters.

It can be concluded that in the experiment, the threshold exceeded the ablation threshold of titanium dioxide during lasering, and it was sufficient in its removal. Titanium dioxide did not interfere with QR code recognition, which was performed with a mobile phone.

It was found that ablation with UV248 laser and Femto laser did not cause a qualitative change in the material during laser marking. The UV248 laser is a laser for laboratory use, while Femto lasers are commonly used in the industry. However, the higher repetition rate of the Femto laser allows faster and more efficient coding, which has key importance in the production. Furthermore, the results show that due to the high performance in the fs pulse length, the wavelength is no longer a critical parameter as it is for ns or longer pulses. The thermal effects are negligibly low in the fs region even at high peak powers. The thermal effects of laser ablation can be avoided by reducing the wavelength or the impulse length based on the current study.

It is known that the efficient use of this technology requires further development in speed. Other high energy near-infrared pulse lasers that operate at multi-kHz versions (with a repetition frequency of multi ten-kHz and also MHz), could potentially further shorten the ablation time. Those devices could even be used for line speed marking in pharmaceutical companies. Also, these devices are scalable in energy and they are capable of implementing the one-shot technique. Further research is needed in this direction by testing new lasers and new techniques.

In conclusion, we propose a functionally advanced marking by the lasers mentioned in this article, highlighting the Femto laser as a solution for pharmaceutical companies that would like to have additional protection against drug counterfeiters or to label personalized medicines, knowing that the technique needs further improvement.

CRediT authorship contribution statement

Krisztina Ludasi: Conceptualization, Data curation, Writing - original draft, Investigation. **Orsolya Jójárt-Laczkovich:** Data curation, Investigation. **Tamás Sovány:** Formal analysis. **Béla Hopp:** Methodology, Supervision. **Tamás Smausz:** Methodology, Investigation. **Attila Andrásik:** Investigation, Visualization. **Tamás Gera:** Investigation, Visualization. **Zsolt Kovács:** Investigation. **Géza Regdon jr:** Writing -

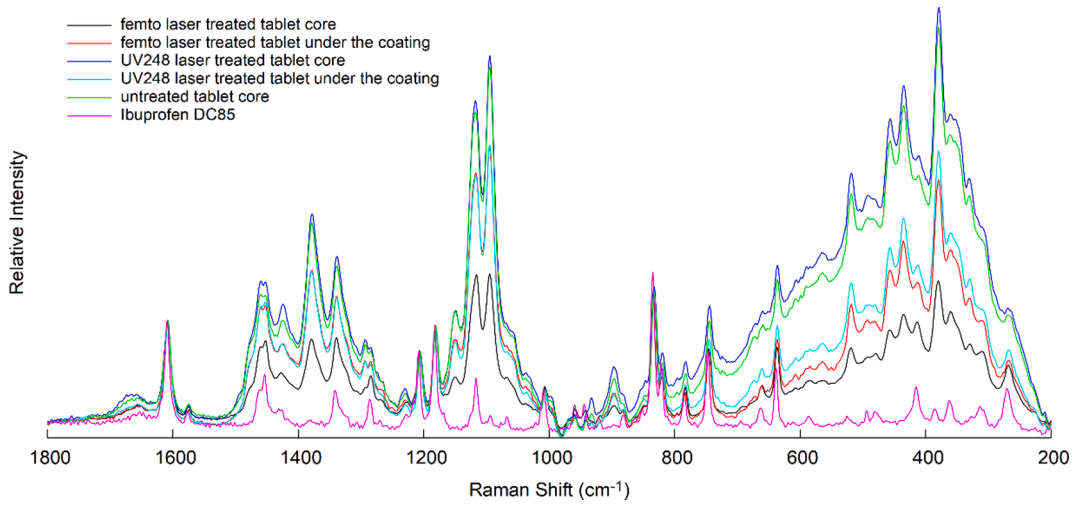

Fig. 15. Averaged and normalised (to Ibu peak 1604 cm^{-1}) spectra taken from the lasered and non-lasered places (both Femto and UV248 laser-treated tablets), spectra of untreated tablet core and Ibuprofen DC85 spectrum.

review & editing, Supervision.

Declaration of Competing Interest

The authors declare that they have no known competing financial interests or personal relationships that could have appeared to influence the work reported in this paper.

Acknowledgement

I would like to thank Seppic S.A. for supplying the polymers.

This work was supported by the EU-funded Hungarian grant EFOP-3.6.1-16-2016-00008.

References

Álvarez, C., Núñez, I., Torrado, J.J., Gordon, J., Potthast, H., García-Arieta, A., 2011. Investigation on the possibility of biowaivers for ibuprofen. J. Pharm. Sci. 100, 2343–2349. https://doi.org/10.1002/jps.22472.

Ayyoubi, S., Cerda, J.R., Fernández-garcía, R., Knief, P., Lalatsa, A., Healy, A.M., Serrano, D.R., 2021. 3D printed spherical mini-tablets: Geometry versus composition effects in controlling dissolution from personalised solid dosage forms. Int. J. Pharm. 120336 https://doi.org/10.1016/j.ijpharm.2021.120336.

Brickell, C.D., 2001. New introductions and the use of genetic resources. Acta Hortic. 552, 159–163. https://doi.org/10.17660/actahortic.2001.552.17.

Dansereau, R., Brock, M., Redman-Furey, N., 1993. The Solubilization of Drug and Excipient Into a Hydroxypropyl Methylcellulose (Hpmc)-Based Film Coating As a Function for the Coating Parameters in a 24“ Accela-Cotab. Drug Dev. Ind. Pharm. 19, 793–808.

Davison, M., 2011. Pharmaceutical Anti-Counterfeiting Combating the Real Danger from Fake Drugs. John Wiley & Sons Inc, Publication, pp. 103–140.

Denso Wave, 1994. QR code development story [WWW Document]. Denso Wave Technol. URL https://www.denso-wave.com/en/technology/vol1.html (accessed 10.6.20).

Dong, Y., Lin, H., Abolghasemi, V., Gan, L., Zeitler, J.A., Shen, Y.C., 2017. Investigating Intra-Tablet Coating Uniformity With Spectral-Domain Optical Coherence Tomography. J. Pharm. Sci. 106, 546–553. Doi: http://dx.doi.10.1016/j.xphs.2016.09.021.

Kannatey-Asibu Jr., E. 2009. Principles of Laser Materials Processing, John Wiley&Sons.

Edinger, M., Bar-Shalom, D., Sandler, N., Rantanen, J., Genina, N., 2018. QR encoded smart oral dosage forms by inkjet printing. Int. J. Pharm. 536, 138–145. https://doi.org/10.1016/j.ijpharm.2017.11.052.

Elliott, D.J., 1995. Ultraviolet Laser Technology and Applications, Ultraviolet Laser Technology and Applications. Doi: http://dx.doi.10.1016/c2009-0-21234-7.

European Commission, 2015. Regulations Commission Delegated Regulation (EU) 2016/161 of 2 October 2015 supplementing Directive 2001/83/EC of the European Parliament and of the Council by laying down detailed rules for the safety features appearing on the packaging medicinal product. Off. J. Eur. Union. Doi: http://dx.doi.10.1017/CBO9781107415324.004.

European Medicines Agency, 2018a. Human regulatory,Owerview, Public health threats, Falsified medicines [WWW Document]. URL http://www.ema.europa.eu/ema/index.jsp?curl=pages/special_topics/general/general_content_000186.jsp&mid=WC0b01ac058002d4e8 (accessed 5.8.19).

European Medicines Agency, 2018b. Mobile scanning and other technologies in the labelling and package leaflet of centrally authorised medicinal products [WWW Document]. URL https://www.ema.europa.eu/en/documents/regulatory-procedural-guideline/mobile-scanning-other-technologies-labelling-package-leaflet-centrally-authorised-medicinal-products_en.pdf (accessed 1.6.21).

F. Menges, 2020. Spectragryph - optical spectroscopy software, Version1.2.15 2020, http://www.effemm2.de/spectragryph/.

Fittler, A., Vida, R.G., Káplár, M., Botz, L., 2018a. Consumers turning to the internet pharmacy market: Cross-sectional study on the frequency and attitudes of hungarian patients purchasing medications online. J. Med. Internet Res. 20, 1–11. Doi: http://dx.doi.10.2196/11115.

Fittler, A., Vida, R.G., Rádics, V., Botz, L., 2018b. A challenge for healthcare but just another opportunity for illegitimate online sellers: Dubious market of shortage oncology drugs. PLoS One 13, 1–17. https://doi.org/10.1371/journal.pone.0203185.

Fukuchi, K., 2020. Libqrencode - a fast and compact QR Code encoding library, v.4.1.1. [WWW Document]. URL https://github.com/fukuchi/libqrencode (accessed 1.11.21).

Guo, H.X., Heinämäki, J., Yliruusi, J., 2002. Diffusion of a freely water-soluble drug in aqueous enteric-coated pellets. AAPS PharmSciTech 3, 8. https://doi.org/10.1208/pt030216.

Haaser, M., Gordon, K.C., Strachan, C.J., Rades, T., 2013. Terahertz pulsed imaging as an advanced characterisation tool for film coatings - A review. Int. J. Pharm. 457, 510–520. https://doi.org/10.1016/j.ijpharm.2013.03.053.

Han, S., Bae, H.J., Kim, J., Shin, S., Choi, S.E., Lee, S.H., Kwon, S., Park, W., 2012a. Lithographically encoded polymer microtaggant using high-capacity and error-correctable QR Code for anti-counterfeiting of drugs. Adv. Mater. 24, 5924–5929. https://doi.org/10.1002/adma.201201486.

Han, S., Bae, H.J., Kim, J., Shin, S., Kwon, S., Park, W., 2012b. Drug authentication using high capacity and error-correctable encoded microtaggants. In: Proc. 16th Int. Conf. Miniaturized Syst. Chem. Life Sci. MicroTAS, pp. 1429–1431.

Ho, L., Müller, R., Römer, M., Gordon, K.C., Heinämäki, J., Kleinebudde, P., Pepper, M., Rades, T., Shen, Y.C., Strachan, C.J., Taday, P.F., Zeitler, J.A., 2007. Analysis of sustained-release tablet film coats using terahertz pulsed imaging. J. Control. Release 119, 253–261. https://doi.org/10.1016/j.jconrel.2007.03.011.

Lawrence, J. (Ed.), 2010. Advances in Laser Materials Processing Technology, Research and Application, Woodhead Publishing Limited. Woodhead Publishing. Doi: http://dx.doi.10.1163/18750176-90000221.

Ludasi, K., Jójárt-Laczkovich, O., Sovány, T., Hopp, B., Smausz, T., Regdon, G., 2019. Comparison of conventionally and naturally coloured coatings marked by laser technology for unique 2D coding of pharmaceuticals. Int. J. Pharm. 570 https://doi.org/10.1016/j.ijpharm.2019.118665.

Ludasi, K., Sovány, T., Laczkovich, O., Hopp, B., Smausz, T., Regdon, G., 2018. Unique laser coding technology to fight falsified medicines. Eur. J. Pharm. Sci. 123 https://doi.org/10.1016/j.ejps.2018.07.023.

Roth, L., Biggs, K.B., Bempong, D.K., 2019. Substandard and falsified medicine screening technologies. AAPS Open 5. https://doi.org/10.1186/s41120-019-0031-y.

Sacher, S., Wahl, P., Weißensteiner, M., Wolfgang, M., Pokhilchuk, Y., Looser, B., Thies, J., Raffa, A., Khinast, J.G., 2019. Shedding light on coatings: Real-time monitoring of coating quality at industrial scale. Int. J. Pharm. 566, 57–66. https://doi.org/10.1016/j.ijpharm.2019.05.048.

Steen, W., Mazumder, J., 2010. Laser Material Processing, 4th ed. Springer. Doi: http://dx.doi.10.1007/978-1-84996-062-5.

Szatmári, S., 1994. High-brightness ultraviolet excimer lasers. Appl. Phys. B Laser Opt. 58, 211–223. https://doi.org/10.1007/BF01081313.

Szatmári, S., Schäfer, F.P., 1988. Simplified laser system for the generation of 60 fs pulses at 248 nm. Opt. Commun. 68, 196–202. Doi: http://dx.doi.10.1016/0030-4018(88)90184-8.

TeWaTi, 2019. TeraWatt Titan-Sapphire Laser Research Group [WWW Document]. URL www.tewati.eu (accessed 6.11.20).

The European Parlament and the Council of the European Union, 2011. Directive 2011/62/EU of the European Parliament and of the Council of 8 June 2011. Off. J. Eur. Union L 174 (74), 74–87.

Trenfield, S.J., Xian Tan, H., Awad, A., Buanz, A., Gaisford, S., Basit, A.W., Goyanes, A., 2019. Track-and-trace: Novel anti-counterfeit measures for 3D printed personalized drug products using smart material inks. Int. J. Pharm. 567 https://doi.org/10.1016/j.ijpharm.2019.06.034.

Van Overschelde, O., Dinu, S., Guisbiers, G., Monteverde, F., Nouvellon, C., Wautelet, M., 2006. Excimer laser ablation of thin titanium oxide films on glass. Appl. Surf. Sci. 252, 4722–4727.

Viswanathan, P., Muralidaran, Y., Ragavan, G., 2017. Challenges in oral drug delivery: A nano-based strategy to overcome. Nanostruct. Oral Med. 173–201 https://doi.org/10.1016/B978-0-323-47720-8.00008-0.

WHO, 2018. Substandard and falsified medical products [WWW Document]. URL https://www.who.int/en/news-room/fact-sheets/detail/substandard-and-falsified-medical-products (accessed 1.9.21).

WHO, 2017a. WHO Global Surveillance and Monitoring System [WWW Document]. URL http://www.who.int/medicines/regulation/ssffc/publications/gsms-report-sf/en/ (accessed 1.9.21).

WHO, 2017b. Seventieth World Health Assembly Update [WWW Document]. Who. URL http://www.who.int/mediacentre/news/releases/2017/dementia-immunization-refuguees/en/ (accessed 1.9.21).

Wilson, K.E., Crossman, E., 1997. The influence of tablet shape and pan speed on intra-tablet film coating uniformity. Drug Dev. Ind. Pharm. 23, 1239–1243. https://doi.org/10.3109/03639049709146164.

Wolfgang, M., Peter, A., Wahl, P., Markl, D., Zeitler, J.A., Khinast, J.G., 2019. At-line validation of optical coherence tomography as in-line/at-line coating thickness measurement method. Int. J. Pharm. 572, 118766 https://doi.org/10.1016/j.ijpharm.2019.118766.